Chen et al. Progress in Earth and Planetary Science (2021) 8:23
https://doi.org/10.1186/s40645-021-00416-9

Progress in Earth and Planetary Science

RESEARCH ARTICLE Open Access

A potential suite of climate markers of long-chain *n*-alkanes and alkenones preserved in the top sediments from the Pacific sector of the Southern Ocean

Xin Chen[1,2*], Xiaodong Liu[1], Da-Cheng Lin[3,4,5], Jianjun Wang[2], Liqi Chen[2], Pai-Sen Yu[6], Linmiao Wang[7], Zhifang Xiong[7] and Min-Te Chen[3,4,5,8*]

Abstract

Investigating organic compounds in marine sediments can potentially unlock a wealth of new information in these climate archives. Here, we present pilot study results of organic geochemical features of long-chain *n*-alkanes and alkenones and individual carbon isotope ratios of long-chain *n*-alkanes from a newly collected, approximately 8 m long, located in the far reaches of the Pacific sector of the Southern Ocean. We analyzed a suite of organic compounds in the core. The results show abundant long-chain *n*-alkanes (C_{29}–C_{35}) with predominant odd-over-even carbon preference, suggesting an origin of terrestrial higher plant waxes via long-range transport of dust, possibly from Australia and New Zealand. The $\delta^{13}C$ values of the C_{31} *n*-alkane range from −29.4 to −24.8‰, in which the higher $\delta^{13}C$ values suggest more contributions from C_4 plant waxes. In the analysis, we found that the mid-chain *n*-alkanes (C_{23}–C_{25}) have a small odd-over-even carbon preference, indicating that they were derived from marine non-diatom pelagic phytoplankton and microalgae and terrestrial sources. Furthermore, the C_{26} and C_{28} with lower $\delta^{13}C$ values (~−34‰) indicate an origin from marine chemoautotrophic bacteria. We found that the abundances of tetra-unsaturated alkenones ($C_{37:4}$) in this Southern Ocean sediment core ranges from 11 to 37%, perhaps a marker of low sea surface temperature (SST). The results of this study strongly indicate that the $\delta^{13}C$ values of long-chain *n*-alkanes and U^k_{37} index are potentially useful to reconstruct the detailed history of C_3/C_4 plants and SST change in the higher latitudes of the Southern Ocean.

Keywords: Southern Ocean, Pacific Ocean, *n*-alkane, Carbon isotopic, SSTU^k_{37}

1 Introduction

The Southern Ocean plays an important role in global climate and the carbon cycle related to westerly winds and the Antarctic Circumpolar Current (ACC, Fischer et al. 2010; Marshall and Speer 2012). Mid-latitude westerly winds are essential in transporting mineral dust from the continent of Australia and New Zealand to the South Pacific sector of the Southern Ocean (Lamy et al. 2014). The westerly winds and ACC's location and intensity directly control the exchange of heat, salt, nutrients, and freshwater between low and high latitudes (Pahnke and Zahn 2005; Toggweiler and Russell 2008; Shevenell et al. 2011; Toyos et al. 2020). Thus, environmental fluctuations in the Southern Ocean play a vital role in global climate change.

Well-preserved organic matter in marine sediments is a direct indicator of environmental conditions at the time of sedimentation and thus is important for paleo-

* Correspondence: chenxust@mail.ustc.edu.cn; mtchen@mail.ntou.edu.tw
[1]Anhui Province Key Laboratory of Polar Environment and Global Change, School of Earth and Space Sciences, University of Science and Technology of China, Hefei 230026, Anhui, China
[3]Institute of Earth Sciences, National Taiwan Ocean University, Keelung 20224, Taiwan
Full list of author information is available at the end of the article

environmental studies (Meyers and Ishiwatari 1993). Among these, lipid organic biomarkers have been widely used to reconstruct past environmental and climatic conditions in oceans and lakes (Eglinton and Eglinton 2008; Holtvoeth et al. 2019). Long-chain *n*-alkanes (C_{25}–C_{35}) are important components of the epicuticular wax in higher terrestrial plants, and these *n*-alkanes are eroded from leaf surfaces and soil by winds and then transported to the Southern Ocean (Bendle et al. 2007; Martínez-Garcia et al. 2009, 2011; Lamy et al. 2014; Jaeschke et al. 2017). Short- and mid-chain lengths are the major components of *n*-alkanes in the surface ocean sediments around Antarctica. These compounds are mainly derived from phytoplankton and bacteria based on carbon preference index (CPI) and specific-compound carbon isotopic values (Harada et al. 1995; Bubba et al. 2004). Relatively high carbon isotopic values of C_{31} *n*-alkane in the surface sediments from the Australian sector of the Southern Ocean suggest significant contributions of C_4 higher vascular plant waxes or conifer resin (Ohkouchi et al. 2000). Altered or recycled material mixed with modern marine input is also an important source for long-chain *n*-alkanes with low CPI values in ocean sediments in the Ross Sea region (Kvenvolden et al. 1987; Venkatesan 1988; Duncan et al. 2019). Although the high latitudes of the Southern Ocean are usually considered to be little influenced by river and continent soils, based on the above results, the sources of *n*-alkanes in the ocean sediments are thought to be complicated; thus, their eco-environmental implications are still being explored.

Subtropical to polar sea surface temperature (SST) gradient has been related to the position and intensity of the westerly winds and ACC in the Southern Ocean (Lamy et al. 2010; Kohfeld et al. 2013). Therefore, quantitative SST records from the past are essential for evaluating the importance of the Southern Ocean for the global climate. However, the most widely used organic geochemical SST index, alkenone paleothermometry, has only rarely been employed in high latitudes of the Southern Ocean. The U^{k}_{37} = ([$C_{37:2}$ − $C_{37:4}$]/[$C_{37:2}$ + $C_{37:3}$ + $C_{37:4}$]) index has been proposed to quantify the degree of alkenone unsaturation (Brassell et al. 1986), which is a function of SST. Because $C_{37:4}$ is often absent in open ocean sediments when SSTs are higher than 12 °C (Prahl and Wakeham 1987), the index was simplified to $U^{k'}_{37}$ = ([$C_{37:2}$]/[$C_{37:2}$ + $C_{37:3}$]). In recent decades, the $U^{k'}_{37}$ index has been widely used in middle and low latitude marine environments. However, our knowledge on the application of alkenone paleothermometry in the high latitudes of the Southern Ocean is still largely insufficient. A few examples exist, such as that $C_{37:4}$ methyl alkenone was not detected in the 10–12 °C waters. Even in the 1.5 °C waters, the abundance was still very minor (Sikes and Volkman 1993), while it was detected in most surface sediment samples at 3.5 °C in spring cruise samples in the Southern Ocean (Sikes et al. 1997). The relative abundance of $C_{37:4}$ alkenone in the surface sediments showed no significant relationship with modern SST, suggesting that $U^{k'}_{37}$ index may be more proper than U^{k}_{37} when used in sea surface temperature estimations, even in cold conditions (Sikes et al. 1997; Jaeschke et al. 2017). However, Ho et al. (2012) found that U^{k}_{37} records display better agreement with planktic foraminifera $\delta^{18}O$ and other SST records at the same sites, suggesting that U^{k}_{37} is more suitable for SST reconstructions in the subantarctic Pacific. Data on alkenone paleothermometry is still largely lacking, and these various results of U^{k}_{37} and $U^{k'}_{37}$ -SSTs indicate that more investigations are still needed in the high latitudes of the Southern Ocean.

Considering the importance of the position and strength of westerly winds and the Antarctic Circumpolar Current, reconstructing surface ocean hydroclimatic changes using organic biomarkers (e.g., long-chain *n*-alkanes and alkenones) is necessary to better understand the role of the Southern Ocean in the context of global climate change. Before carrying out such work, it is crucial to determine the source of organic matter and to estimate whether U^{k}_{37} index could be useful or not in the Southern Ocean. Here, we analyze the organic geochemical features of long-chain *n*-alkanes, alkenones, and the compound-specific carbon isotope of long-chain *n*-alkanes (C_{23}–C_{31}) in the ocean sediments from one core in the South Pacific sector of the Southern Ocean (R23, 66° 13′ 47.16″ S, 168° 11′ 8.34″ E). Our main objectives are (a) to evaluate the source of long-chain *n*-alkanes based on their chain length distributions and individual carbon isotopes, (b) to report the distributional features of di-, tri-, and tetra-unsaturated alkenone, and (c) to assess the applicability of the alkenone indices in the high latitudes of the Southern Ocean for reconstructing past climate changes.

2 Materials and methods

2.1 Materials

The gravity core R23 was drilled at 168° 11′ 8.34″ E, 66° 13′ 47.16″ S at a water depth of 2967 m during the "31th Chinese National Antarctic Research Expedition (CHINARE)" cruise in 2014–2015 (Fig. 1). The sediment core is 819 cm long, with a top 10 cm soupy layer characterized by high water content. The core was subsampled at an interval of 2 cm. The color of the sediments varies among olive, brown, and gray throughout the profile. Based on the wet and dry sieving experiments, the core mainly consists of homogenous clay with minor proportion of sand (63–2000 μm), some ice-rafted debris

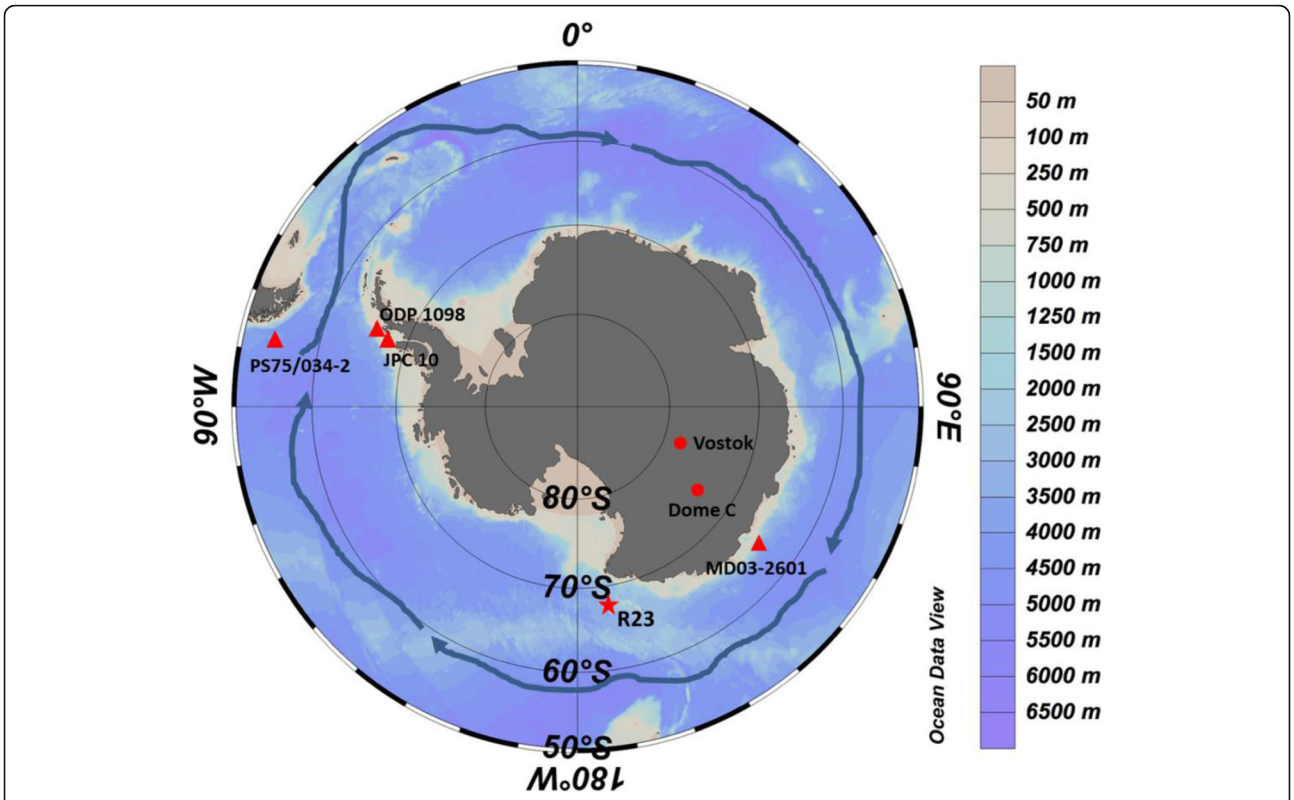

Fig. 1 Map of the Southern Ocean and the continent of Antarctica. The red pentagram denotes the core R23 in our study. Red triangles indicate sites of sea surface temperature or sea subsurface temperature records reported in previous studies. The SST record in the PS75/034-2 sediment core was used for the U^{k}_{37} index (Ho et al. 2012), whereas other sediment cores (ODP 1098, JPC 10, and MD03-2601) were used for TEX_{86} (Shevenell et al. 2011; Kim et al. 2012; Etourneau et al. 2013). The thick blue line indicates the Antarctic Circumpolar Current (ACC). The solid dots denote ice core locations in the Antarctic, including Dome C and Vostok

(IRD; >2 mm), and some foraminifera randomly found, but sponge spicules are present throughout the core with relatively high abundance. No obvious bioturbations were observed in this core. In this pilot study, we only focus on the source identification of *n*-alkanes with different chain lengths and then evaluate the possibility of C_{37} alkenones used as a suitable proxy for calculating the past sea surface temperature in this region. To study the potential of sedimentary organic geochemical features for paleoclimate reconstruction, we choose 12 samples at every ~ 80 cm interval for *n*-alkane and alkenone analysis in this pilot study. All samples were stored under −20°C in the lab before analysis.

2.2 Lipid biomarker extraction

The lipid analysis procedure followed the methods of Yamamoto et al. (2000). Briefly, all sediment samples were freeze-dried and then homogenized and powdered. Samples (2–3 g) were weighed and extracted two times with an Accelerated Solvent Extractor (DIONEX ASE 350) using dichloromethane-methanol (6:4 v/v) and then concentrated. The total lipid extract was separated into four fractions using column chromatography (SiO_2 with 5% distilled water; internal diameter, 5.5 mm; length, 45 mm) based on the degree of polarity: F1 (hydrocarbons, 4 ml hexane); F2 (aromatic hydrocarbons, 4 ml hexane-toluene (3:1 v/v)); F3 (ketones, 4 ml toluene); F4 (polar compounds, 4 ml toluene-methanol (3:1 v/v)). *N*-$C_{24}D_{50}$ and *n*-$C_{36}H_{74}$ were added as internal standards for the F1 and F3 fraction, respectively. Compounds were quantified using an internal standard *n*-$C_{24}D_{50}$ and *n*-$C_{36}H_{74}$ for *n*-alkanes and alkenones, respectively.

2.3 *n*-alkane and alkenone analysis

Quantification of compounds was performed on a Hewlett Packard 6890 GC-FID system with a Chrompack DB-1MS column (length, 60 m; i.d., 0.25 mm; thickness, 0.25 μm). The oven temperature was programmed from 70 to 290 °C at 20 °C/min, 290 to 310 °C at 0.5 °C/min, and then held at 310 °C for more than 30 min. Helium was used as the carrier gas, with a flow rate of 30 cm/s. Selected samples were performed using GC-MS for compound identification. The GC column and oven temperature program were the same as GC-FID. The mass spectrometer was run in full scan mode (m/z 50–650). Electron ionization (EI) spectra were obtained at

70 eV. Alkenones were identified using an external standard by GC retention times by analogy with a synthetic standard (provided by M. Yamamoto, Hokkaido University, Japan) and characteristic mass fragments. *N*-alkanes were identified by comparing mass spectra and retention times with those of the standards and published data.

The carbon preference index (CPI; Bray and Evans 1961) of C_{26}–C_{34} homologs and the average chain length (ACL) of odd C_{27}–C_{35} homologs (Duan and He 2011) used in this study were as follows:

$$\mathrm{CPI} = \left(\frac{C_{27}+C_{29}+C_{31}+C_{33}}{C_{26}+C_{28}+C_{30}+C_{32}} + \frac{C_{27}+C_{29}+C_{31}+C_{33}}{C_{28}+C_{30}+C_{32}+C_{34}}\right)/2 \quad (1)$$

$$\mathrm{ACL} = \frac{27\times C_{27}+29\times C_{29}+31\times C_{31}+33\times C_{33}+35\times C_{35}}{C_{27}+C_{29}+C_{31}+C_{33}+C_{35}} \quad (2)$$

The $[C_{26}$–$C_{35}]$ are concentrations of odd and even *n*-alkane. The U^{k}_{37} = ($[C_{37:2}$–$C_{37:4}]/[C_{37:2}$ + $C_{37:3}$ + $C_{37:4}]$) index has been proposed to quantify the degree of alkenone unsaturation (Brassell et al. 1986), which is a function of SST. Because $C_{37:4}$ is often absent in open ocean sediments when SSTs are higher than 12 °C (Prahl and Wakeham 1987), the index was simplified to $U^{k'}_{37}$ = ($[C_{37:2}]/[C_{37:2}$ + $C_{37:3}]$). We converted the index values to SST using the widely used *Emiliania huxleyi* culture-based calibration proposed by Prahl et al. (1988), U^{k}_{37} = 0.04 T − 0.104 (r^2 = 0.98) and $U^{k'}_{37}$ = 0.034 T + 0.039 (r^2 = 0.99), and the simplified $U^{k'}_{37}$ calibration was based on global core top compilations (Conte et al. 2006).

2.4 Carbon isotope analysis

The carbon isotope ratio of *n*-alkanes was performed using a gas chromatograph with a DB-5MS column (60 m × 320 μm × 250 μm) interfaced to a Thermo Scientific MAT-253 isotope-ratio mass spectrometer via a combustion interface (960 °C) consisting of an alumina reactor containing nickel and platinum wires. Helium was used as the carrier gas with a flow rate of 1.2 ml/min using splitless injecting. The oven temperature was programmed from 80 to 100 °C at 10 °C/min, 100 to 220 °C at 4 °C/min, 220 to 280 °C at 2 °C/min, and then held at 280 °C for 15 min. All samples are injected one time for carbon isotope analysis. The analytical error was calculated based on the reproduced analytical results of an external standard, injected once after every sixth sample injection, and had an analytical error of 0.7‰ (1σ). The pre-calibrated isotopic composition of CO_2 was used as a standard. All $\delta^{13}C$ values were expressed versus VPDB.

Based on the isotopic values of *n*-alkanes, we can quantify the percentage source of long-chain *n*-alkanes from C_3/C_4 plants using a binary isotope mass balance model (Thomas et al. 2014):

$$\delta^{13}C_S = f\times\delta^{13}C_{C3} + (1-f)\times\delta^{13}C_{C4} \quad (3)$$

where $\delta^{13}C_s$ is the long-chain *n*-alkanes from sediments, $\delta^{13}C_{C3}$ and $\delta^{13}C_{C4}$ are the carbon isotopic values of long-chain *n*-alkanes from C_3 and C_4 terrestrial higher vascular plants, respectively, and *f* is the proportion of long-chain *n*-alkanes from C_3 plants. We set the carbon isotopic values of long-chain *n*-alkanes for C_3 and C_4 plants to be −36‰ and −22‰, respectively (Chikaraishi and Naraoka 2007; Vogts et al. 2009). C_{31} *n*-alkane abundance is relatively higher than C_{29} and C_{33} *n*-alkanes; thus, we use the carbon isotopic values of C_{31} *n*-alkane to calculate the percentage source of long-chain *n*-alkanes from C_3/C_4 plants.

3 Results

3.1 Concentration and distribution of long-chain *n*-alkanes

In the 12 pilot samples from the core R23, we found a significant change in the concentrations of total long-chain *n*-alkanes (C_{23}–C_{35}) in the sediment profile, ranging from 295–787 ng/g sediment dry weight (Table 1, Table S1, Fig. 2). The distribution pattern of long-chain *n*-alkanes (C_{23}–C_{35}) in each sediment sample was similar, with bimodal distributions peaking at C_{23}–C_{25} and C_{27} or C_{31} (Fig. 3). However, there was no apparent predominant odd-over-even carbon preference, and CPI_{27-33} varied from 1.1 to 2.5, with an average of 1.7 (Fig. 2). The distribution patterns of long-chain *n*-alkanes were divided into two types. One is mid-chain *n*-alkanes (C_{23}–C_{27}), with no predominant odd-over-even carbon preference (CPI ~1), and the other is long-chain *n*-alkanes (C_{29}–C_{35}) with dominant odd-over-even carbon preference. The ACL values of long-chain *n*-alkanes (C_{27}–C_{35}) were in the range of 29.3–30.7. The ACL values are strongly correlated with CPI (Fig. 4).

3.2 Concentration and distribution of alkenones

$C_{37:4}$, $C_{37:3}$, and $C_{37:2}$ alkenones were all detected in the 12 pilot samples, with total concentrations ranging from 12.6 to 104.2 ng/g sediment dry weight (Table 2). The distribution pattern of three unsaturated alkenones revealed significant differences among the subsamples, and the relative abundance of $C_{37:4}$, $C_{37:3}$, and $C_{37:2}$ varied from 11 to 37%, 27 to 87%, and 3 to 48%, respectively. The tri-unsaturated alkenone ($C_{37:3}$) was the most abundant in the sediments. Interestingly, a high abundance of tetra-unsaturated alkenone was found in the sediment samples. The SST estimates we inferred from the U^{k}_{37}

Table 1 Concentrations, $\delta^{13}C$ values, and typical indices based on *n*-alkanes in the subsamples with different sediment depth of core R23. The relative contribution of long chain *n*-alkanes from C_3 and C_4 plants are calculated by carbon isotopes of the C_{31} *n*-alkane

Depth (cm)	$\delta^{13}C_{23}$ (‰)	$\delta^{13}C_{24}$ (‰)	$\delta^{13}C_{25}$ (‰)	$\delta^{13}C_{26}$ (‰)	$\delta^{13}C_{27}$ (‰)	$\delta^{13}C_{28}$ (‰)	$\delta^{13}C_{29}$ (‰)	$\delta^{13}C_{31}$ (‰)	*n*-alkanes[a] (ng/g)	C_4 (%)	C_3 (%)	ACL[b]	CPI[c]
16	−29.6	−28.8	−29.9	−33.2	−28.5	−32.2	−27.4	−28.3	445	55	45	30.1	1.6
88	−29.5	−31.8	−27.3	−30.0	−26.3	−33.1	−25.1	−25.5	328	75	25	30.3	2.0
166	−25.4	−26.4	−26.7	−32.5	−28.3	−38.0	−27.1	−27.8	295	59	41	30.1	2.1
243	−27.1	−26.8	−26.8	−30.4	−26.7	−33.3	−29.8	−28.3	362	55	45	30.3	2.5
323	−29.8	−31.2	−30.6	−35.0	−28.3	−32.1	−29.4	−27.9	324	58	42	29.3	1.3
398	−31.5	−35.9	−30.0	−36.7	−28.6	−34.6	−25.0	−24.8	787	80	20	29.6	1.3
482	−26.8	−28.4	−29.3	−30.3	−26.8	−30.1	−27.4	−26.6	411	67	33	30.7	1.9
550	−27.1	−30.7	−29.3	−35.1	−27.8	−31.2	−27.8	−25.4	420	76	24	30.1	1.6
626	−30.4	−32.2	−31.7	−34.6	−29.6	−30.9	−26.4	−25.8	344	73	27	29.6	1.6
698	−28.6	−30.6	−29.0	−32.7	−27.8	−31.8	−27.0	−25.8	490	73	27	29.3	1.1
762	−28.8	−29.3	−30.0	−35.3	−26.7	−32.1	−30.4	−29.4	455	47	53	29.8	1.6
818	−28.8	−28.7	−32.3	−37.4	−30.1	−35.8	−27.7	−27.2	503	63	37	30.1	1.7

[a]Total concentrations of C_{23}-C_{35} *n*-alkanes
[b]$ACL_{27\text{-}35} = \Sigma(i \times X_i)/\Sigma X_i$, where *X* is abundance and *i* ranges from C_{27} to C_{35} odd *n*-alkanes
[c]$CPI_{27\text{-}33} = 0.5 \times \Sigma(C_{27}–C_{33})/(C_{26}–C_{32}) + 0.5 \times \Sigma(C_{27}–C_{33})/(C_{28}–C_{34})$

and $U^{k'}_{37}$ indexes are between −1.7 to 8.4 °C and −0.4 to 17.9 °C, respectively.

3.3 The carbon isotope values of individual *n*-alkanes

Our *n*-alkane-specified carbon isotope analysis of the 12 pilot samples shows a significant change. Therefore, based on the chain length of the *n*-alkanes, we divided *n*-alkanes into two endmembers (Table 1). One is mid-chain *n*-alkanes, which had $\delta^{13}C$ values ranging from −31.5 to −25.4‰ and −32.3 to −26.7‰, with an average of −28.6‰ and −29.4‰ for C_{23} and C_{25}, respectively. The other is long-chain *n*-alkanes (C_{27}, C_{29}, and C_{31}), with $\delta^{13}C$ values from −30.1 to −26.3‰ (C_{27}, averaging −28.0‰), −30.4 to −25.0‰ (C_{29}, averaging −27.5‰), and −29.4 to −24.8‰ (C_{31}, averaging −26.9‰). The average $\delta^{13}C$ values of long-chain *n*-alkanes (C_{27}, C_{29}, and C_{31}) were higher than mid-chain *n*-alkanes (C_{23} and C_{25}). C_{26} and C_{28} *n*-alkanes had the lowest $\delta^{13}C$ values averaging ~ −34‰. The percentage source of long-chain *n*-alkanes

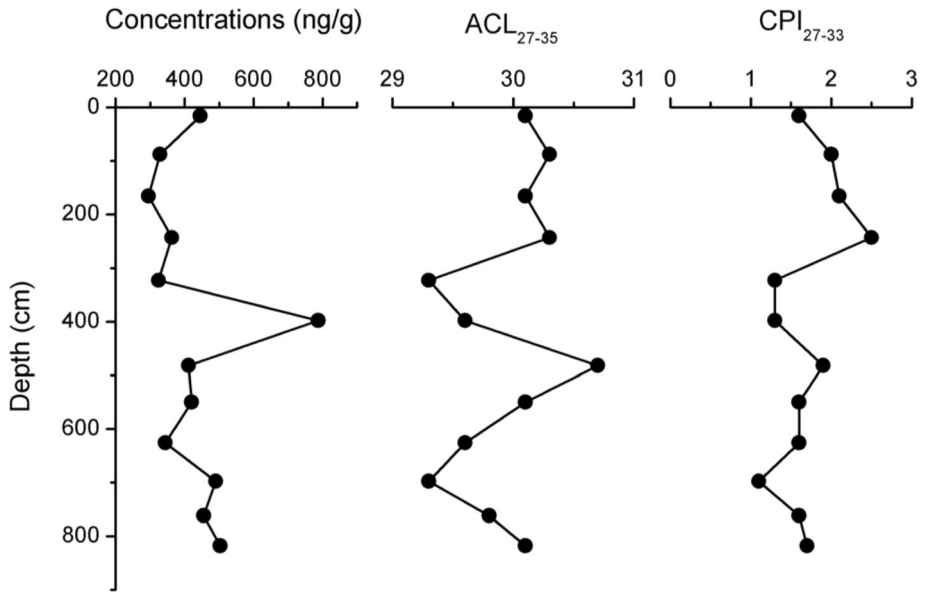

Fig. 2 The concentrations (C_{23}–C_{35}), ACL ($C_{27–35}$–C_{35}), and CPI (C_{27}–C_{33}) values of *n*-alkanes at different depths of the core R23

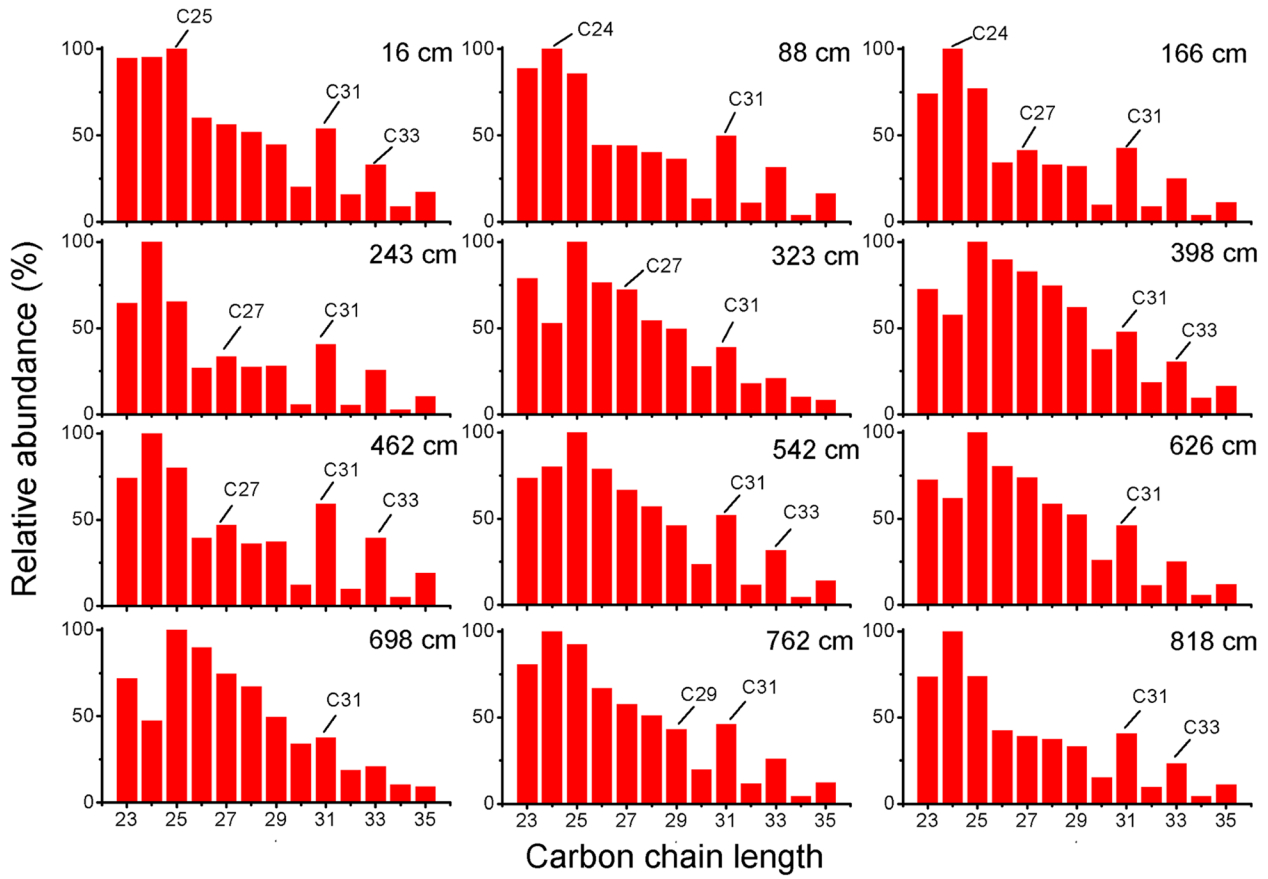

Fig. 3 The relative abundance of long chain *n*-alkanes (C_{23}–C_{35}) at different depths of the core R23

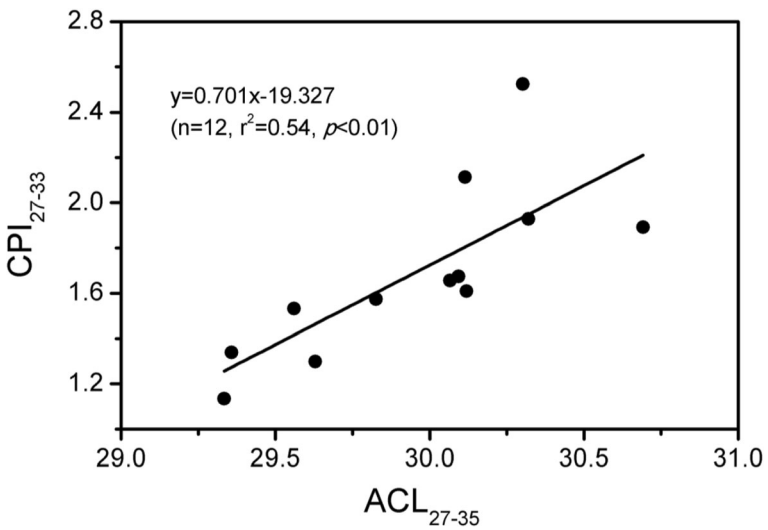

Fig. 4 Relationship between ACL_{27-35} and CPI_{27-33} of long chain *n*-alkanes in the core R23

Table 2 The relative abundance and concentrations of $C_{37:4}$, $C_{37:3}$, and $C_{37:2}$ alkenones and based on U^{k}_{37}- and $U^{k'}_{37}$-SST in the subsamples with different sediment depth of core R23

Depth (cm)	$C_{37:4}$ (%)	$C_{37:3}$ (%)	$C_{37:2}$ (%)	Alkenones (ng/g)	U^{k}_{37}-SST[a] (°C)	$U^{k'}_{37}$-SST[b] (°C)
16	12	85	4	90.7	0.6	−0.1
88	11	87	3	104.2	0.7	−0.4
166	30	40	30	13.2	2.8	11.5
243	21	51	28	15.3	4.4	9.2
323	35	48	17	14.7	−1.7	6.6
398	16	64	19	50.1	3.5	5.6
482	15	80	6	65.1	0.5	0.7
550	37	38	24	12.6	−0.6	10.3
626	30	44	26	14.0	1.8	9.9
698	23	59	18	19.1	1.2	5.7
762	25	27	48	30.2	8.4	17.9
818	30	36	34	19.0	3.6	13.2

[a] $U^{k'}_{37} = C_{37:2}/(C_{37:2}+ C_{37:3})$
[b] $U^{k}_{37} = (C_{37:2}-C_{37:4})/(C_{37:2}+ C_{37:3}+ C_{37:4})$

from C_3/C_4 plants using C_{31} $\delta^{13}C$ values varied from 47 to 80% for C_4 plants (Table 1).

4 Discussion

4.1 Source of mid-chain *n*-alkanes

Our pilot study indicates that the mid-chain *n*-alkanes (C_{23}–C_{25}) are abundant with no predominant odd-over-even carbon preference in the sediment profile (CPI ~1; Fig. 3), and the contamination of petroleum may cause this during coring and sampling. However, our sampling procedures by the crew of the R/V Xuelong in the 31st CHINARE have been devised to prevent any possible contamination by petroleum, and no signs of petroleum contamination have been observed while treating sediment samples in the laboratory. All labware was baked at 450 °C in a furnace before using to prevent contamination during the analysis of the samples. Blank experiments were also analyzed, and negligible contamination was found. Furthermore, the average $\delta^{13}C$ values of *n*-alkanes with different chain lengths are different (Table 1, Fig. 5). For example, the average $\delta^{13}C$ values of mid-chain *n*-alkanes (C_{23}–C_{25}) were similar to the *n*-alkanes from marine phytoplankton (Ashley et al. 2020). Therefore, it is very unlikely that these *n*-alkanes were due to petroleum contamination during coring and sampling. The abundant mid-chain *n*-alkanes (C_{23}–C_{25}) with no predominant odd-over-even carbon preference were natural characteristics in the sediment samples of core R23.

Several studies have shown that ocean phytoplankton can produce mid-chain *n*-alkanes and *n*-alkanoic acids (e.g., Volkman et al. 1998). *N*-alkanoic acids are biosynthesized in the acetogenic pathway, and then, they are converted to *n*-alkanes by enzymatic decarboxylation; thus, they have similar distributions (Diefendorf and Freimuth 2017). Mid-chain *n*-alkanoic acids (C_{22}–C_{24}) can be produced by marine plants, such as marine microalgae, diatoms, and seaweed (Naraoka and Ishiwatari 2000). Therefore, phytoplankton may be a significant

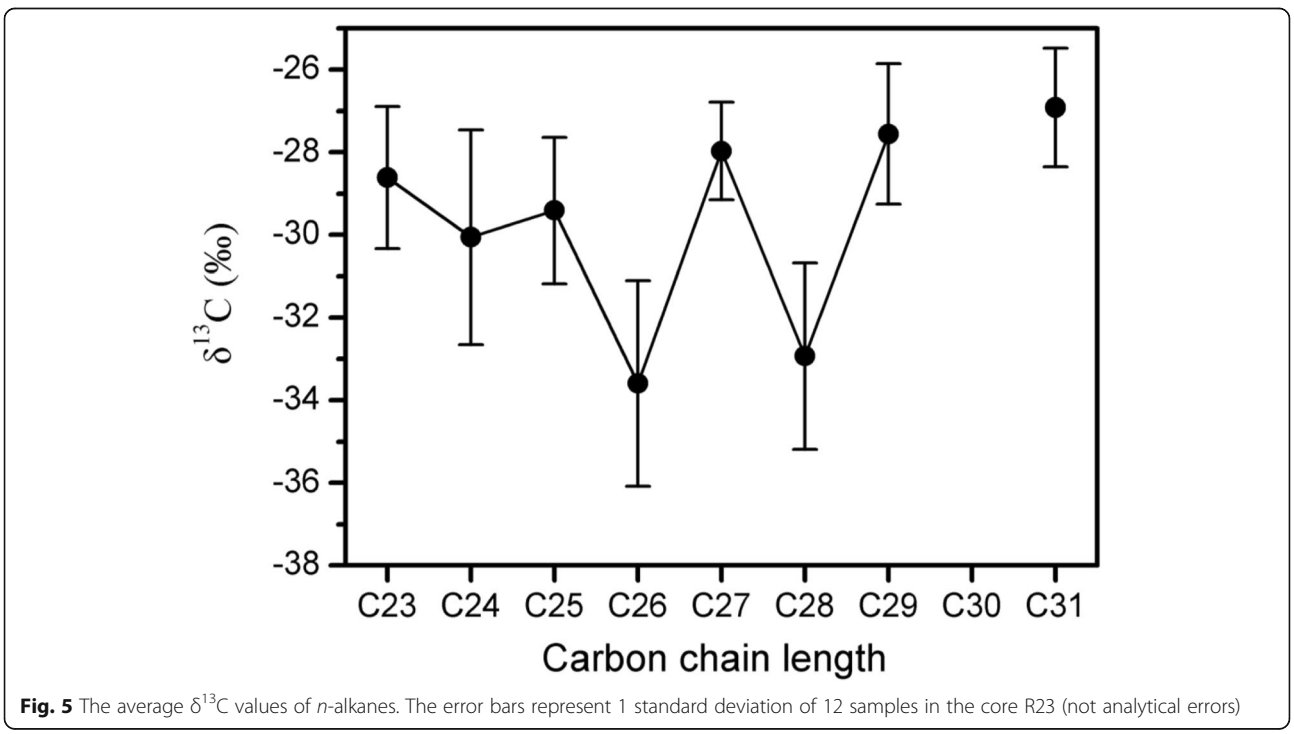

Fig. 5 The average $\delta^{13}C$ values of *n*-alkanes. The error bars represent 1 standard deviation of 12 samples in the core R23 (not analytical errors)

source for these mid-chain *n*-alkanes with no predominant odd-over-even carbon preference (CPI ~ 1). A previous study has reported that the average $\delta^{13}C$ values of *n*-alkanoic acids produced by marine phytoplankton were about −28‰ (Ashley et al. 2020). In our pilot analysis of the 12 samples, the average $\delta^{13}C$ values of *n*-alkanes with different chain lengths vary greatly. The $\delta^{13}C$ values of mid-chain *n*-alkanes (C_{23}–C_{25}; ~ −29‰) are in the range of *n*-alkanes from marine organisms, and soil samples (~−28‰) in the McMurdo Dry Valleys (Hayes et al. 1990; Ishiwatari et al. 1994; Matsumoto et al. 2010), but lower than lake sediments (~−15‰) with shallow water depth from East Antarctica (Chen et al. 2019). Thus, the terrestrial organic matter from ice-free areas of Antarctica transported by ice-rafted debris (IRD) and aeolian may also contribute to mid-chain *n*-alkanes (Chewings et al. 2014). Still, the source from shallow lake sediments at higher latitudes was considered negligible. The $\delta^{13}C$ values of C_{26} and C_{28} are lower than other long-chain *n*-alkanes (Fig. 5), suggesting they may have other sources. Moreover, the $\delta^{13}C$ values of C_{26} and C_{28} in our study samples are also obviously depleted relative to marine organisms and soil samples from Antarctica. The C_{26} and C_{28} may likely originate from chemoautotrophic bacteria because they have relatively low $\delta^{13}C$ values and have no odd-over-even predominance (Hayes et al. 1990; Collister et al. 1994). Thus, from the above discussion, we believe that mid-chain *n*-alkanes (C_{23} to C_{25}) have mixing sources, including marine (non-diatom pelagic phytoplankton and marine microalgae) and terrestrial organic matter, but C_{26} and C_{28} *n*-alkanes might be originated mainly from chemoautotrophic bacteria.

4.2 Sources of long-chain *n*-alkanes

There are three major sources for long-chain *n*-alkanes (C_{27}–C_{35}) in the South Pacific sector of the Southern Ocean sediments, including long-range transport of dust from lower latitudes, ocean plankton, and sediments eroded from Antarctica. Previous studies have shown that short- and mid-chain *n*-alkanes are predominant in Pleistocene age ocean sediments, modern water column-suspended particulate matter in the Ross Sea and Antarctic margin, while long-chain *n*-alkanes have a minor contribution (Harada et al. 1995; Hayakawa et al. 1996; Cincinelli et al. 2008). Moreover, the $\delta^{13}C$ values of *n*-alkanes ranged from −28.5 to −26.2‰, suggesting that their major source was possibly derived from marine organisms (Harada et al. 1995). In the Ross Sea, abundant long-chain *n*-alkanes with low CPI values in ocean sediments have suggested that the organic matter was mainly originated from altered or recycled material mixed with modern marine input (Kvenvolden et al. 1987; Venkatesan 1988; Duncan et al. 2019). Long-range transport of terrestrial organic matter and higher plant leaf waxes is also an important source for long-chain *n*-alkanes in the Pacific sector of the Southern Ocean (Bendle et al. 2007; Martínez-Garcia et al. 2009, 2011; Lamy et al. 2014; Jaeschke et al. 2017). For example, Bendle et al. (2007) studied organic geochemical characteristics in Southern Ocean aerosol samples, and their results showed that the abundant long-chain *n*-alkanes with relatively low $\delta^{13}C$ values (−37 to −30.8‰) represented a regional background of well-mixed higher vascular plants through long-range transportation.

The core R23 is near the Antarctic continent, and so the organic matter from Antarctica may be a potential source of long-chain *n*-alkanes at our site. However, there are no vascular plants in the Antarctic, except for limited terrestrial vegetation (moss and lichen) in relatively low latitudes of the Antarctic Peninsula. Dust contribution from terrestrial material through aeolian transportation is negligible due to the lack of exposed, mature soils in the McMurdo Dry Valleys and Victoria Land (Nylen et al. 2004; Lewis et al. 2008; Lewis and Ashworth 2016), as well as the long-distance of the core site from the coast. Moreover, Matsumoto et al. (2010) have reported that the chain length of *n*-alkanes ranging from C_{15} to C_{37} was found in McMurdo Dry Valley soil, with the majority as C_{23}, C_{25}, and C_{27} *n*-alkanes, but with extremely low abundance of C_{29} and C_{31} *n*-alkanes. Recently, Chen et al. (2019) reported that abundant long-chain *n*-alkanes with highly enriched carbon isotopic ratios (~−25 to −12‰) in shallow lake sediments from East Antarctic (no vascular plants are present in the surrounding landmass) were predominantly derived from heterotrophic microbes. However, the average $\delta^{13}C$ values of long-chain *n*-alkanes (C_{27}, C_{29}, and C_{31}) varying from ~ −28 to −27‰ in the R23 sediments are lower than these in the lacustrine sediments from East Antarctica. Therefore, the sources of long-chain *n*-alkanes (C_{27}–C_{35}) from ice-free soils and shallow lacustrine sediments in East Antarctica via dust transport and ocean phytoplankton is negligible.

The ACL of long-chain *n*-alkanes refers to the average number of carbon atoms/molecule and can indicate their source (Poynter and Eglinton 1990). The ACL values of long-chain *n*-alkanes (C_{27}–C_{35}) ranged from 29.3 to 30.7 in the sediment samples, similar to Southern Ocean ACL values with a range of 29.1–30.6 in the surface sediments, both indicating the significant contribution of higher plants (Jaeschke et al. 2017). A significant linear relationship was observed between ACL and CPI (n = 12, r^2 = 0.54, p < 0.01; Fig. 4). Generally, relatively high CPI values (CPI > 3) indicate long-chain *n*-alkanes from higher vascular plants, while low CPI values (CPI ~1) may imply post-depositional degradation and mature organic matter inputs (Eglinton and Eglinton 2008;

Duncan et al. 2019). According to leaf litter degradation experiments, the odd-over-even predominance of *n*-alkanes was observed to decline. The long-chain *n*-alkane ratios (e.g., C_{31}/C_{29}) were tended to ~ 1 (Zech et al. 2011). Based on this result, it is reasonable to infer that *n*-alkanes in the dust might have experienced a certain degree of degradation during long-range transportation and post-deposition, which could result in low CPI values. Furthermore, relatively low CPI values of 1.1 to 2.5 present in the R23 sediment core may also be considered to microbial degradation under very low sedimentation rates < 2 cm/ka (Tiedemann 2012; Jaeschke et al. 2017; Duncan et al. 2019). Previous studies have shown that the average sedimentation rates were as low as 1.18 cm/ka in Prydz Bay (Wu et al. 2015) and 1.00 cm/ka in ODP 1167 (Theissen et al. 2003). Low CPIs and low sedimentation rates in the DSDP 274 sediment core from the northwest Ross Sea suggest that long-chain *n*-alkanes have been extensively degraded by bacterial activity in the seabed surface layers (Duncan et al. 2019). Under the condition of degradation, the $\delta^{13}C$ values of long-chain *n*-alkanes have no obvious difference (Huang et al. 1997; Li et al. 2017); thus, it could be useful to trace the sources of organic matter and reconstruct the paleoecological changes. The high abundance of long-chain even *n*-alkanes (C_{26} and C_{28}) with lower $\delta^{13}C$ values in the R23 sediment core indicates microbial (chemoautotrophic) activity in this region. Altered or recycled organic matter from Antarctica that has been eroded by glaciers and transported by IRD is important in the study region (Chewings et al. 2014; Duncan et al. 2019). Therefore, we suggest that the long-chain *n*-alkanes (C_{29}–C_{35}) primarily originated from terrestrial higher plant waxes via long-range transport of dust from Australia and New Zealand and altered or recycled organic matter from Antarctica may be another secondary source.

Our results are consistent with previous studies in the Southern Ocean. Long-chain *n*-alkanes were reported to originate mainly from long-range transport of dust from Australia and New Zealand by prevailing westerlies (Martínez-Garcia et al. 2011; Lamy et al. 2014). For example, relatively enriched carbon isotopic ratios of C_{31} *n*-alkane in the surface sediments from the Australian sector of the Southern Ocean suggest significant contributions of C_4 higher vascular plant waxes (Ohkouchi et al. 2000). More recently, Jaeschke et al. (2017) have reported that the CPI values of long-chain *n*-alkanes ranged from 1.1 to 10 in the Pacific sector of the Southern Ocean, indicating the contribution of higher plant leaf waxes. Because the location of surface sediments in our study site is far from the potential source regions (New Zealand and Australia), it is reasonable to believe that the long-chain *n*-alkanes in the R23 sediment core are primarily derived from terrestrial higher plant leaf wax through long-range aeolian transportation.

4.3 Estimation of C_3/C_4 plant fraction

As discussed above, the long-chain *n*-alkanes (C_{27}, C_{29}, and C_{31}) in R23 sediments are primarily derived from higher plant leaf waxes by long-range transport of dust. Interestingly, the $\delta^{13}C$ values of long-chain *n*-alkanes were 5–10‰ higher than those in C_3 plants. This difference indicates that considerable amounts of *n*-alkanes are derived from C_4 plant waxes, which have significantly higher carbon isotopic values. The relative contributions of long-chain *n*-alkanes (C_{27}, C_{29}, and C_{31}) from C_3 and C_4 plants are significantly different in the sediment samples. For the carbon isotopic values of C_{31} *n*-alkanes, 80% originated from C_4 plants in the 398 cm section; however, only 47% originated from C_4 plants in the 762 cm section (Table 1). Ohkouchi et al. (2000) reported that the relative contributions of C_{31} *n*-alkanes from C_3 and C_4 plants are about 60% and 40% in the surface sediments from the Australian sector of the Southern Ocean respectively (Ohkouchi et al. 2000). Previous studies have demonstrated that the primary drivers for the distributions of C_3/C_4 plants are climatic and atmospheric pCO_2 etc. (Huang et al. 2001; Edwards et al. 2010). Compared with C_3 plants, C_4 grasses usually favor relatively lower pCO_2 and arid conditions due to their greater water use efficiency and carbon-concentrating mechanism (Edwards et al. 2010). Therefore, the different contributions of C_3/C_4 plants may be related to climate change (e.g., temperature and precipitation) in the source regions (Huang et al. 2001). Based on the above discussion, it is reasonable to infer that the source of the long-chain *n*-alkanes was mainly derived from long-range transport of dust from New Zealand and Australia (Neff and Bertler 2015). Therefore, these results indicate that the $\delta^{13}C$ values of long-chain *n*-alkanes could be used to reconstruct the past changes of C_3/C_4 plants in the source area and then investigate climatic variations.

4.4 Assessing U^{k}_{37} and $U^{k'}_{37}$-derived SST records

$C_{37:4}$ alkenone was found in the R23 sediments with relative abundance ranging from 11 to 37%. This is similar to a previous study in the higher latitude of the Pacific sector of the Southern Ocean (Sikes et al. 1997) but significantly higher than the sedimentary abundance from the lower latitudes of the Southern Ocean (Jaeschke et al. 2017). Previous studies have shown that $C_{37:4}$ is often absent in open ocean sediments where SSTs are higher than 12 °C (Prahl and Wakeham 1987). The modern annual SST in our study site is about 0 °C; thus, the high abundance of $C_{37:4}$ alkenone may be related to the extremely low temperature. Numerous studies have demonstrated that a high abundance of $C_{37:4}$ in

surface sediments is related to low-temperature and low-salinity surface water masses in the Arctic (Sicre et al. 2002; Bendle et al. 2005; Harada et al. 2006, 2012). Analysis of 106 surface water and sediment samples from the Atlantic, Pacific, and the Southern Ocean indicated that the relative abundance of $C_{37:4}$ methyl alkenone had no apparent relationship with SST and salinity. Still, it might respond to some other environmental factors, including growth rate, light, or nutrients (Sikes and Sicre 2002). For example, $\%C_{37:4}$ showed a negative linear correlation with sea surface salinity (SSS), nutrients, and late summer SST in the suspended particles and sediment profiles from the Bering Sea (Harada et al. 2012). However, SST and SSS showed a strong negative linear relationship in the north Atlantic and the Bering Sea because of sea ice melting during the summer season, suggesting that the strong relationship of $\%C_{37:4}$ and salinity may be the artifact of the good correlation of salinity and temperature (Sikes and Sicre 2002). Moreover, up until now, most samples were from the Atlantic and Pacific Oceans, and there were few studies on the distributional characteristics of alkenones in the high latitudes of the Southern Ocean.

To determine whether SST affects the relative abundance of $C_{37:4}$ methyl alkenone, we calculated the sea surface temperature based on the U^{k}_{37} and $U^{k'}_{37}$ indexes using the formula reported by Prahl et al. (1988) and Conte et al. (2006), respectively (Table 2). Our results show that SST data between U^{k}_{37}- and $U^{k'}_{37}$-SST were, as we expected, obviously different (Fig. 6). When the relative abundance of tetra-unsaturated alkenone was higher, we found that $U^{k'}_{37}$-SST was warmer than U^{k}_{37}-SST in 166, 243, 323, 550, 626, 762, and 818 cm sediment sections, and the difference between $U^{k'}_{37}$ and U^{k}_{37}-SST is in the range of 4.8–10.9 °C. However, the SST difference calculated by these two indexes is relatively small in the sediment sections of the lower abundance of $C_{37:4}$ alkenone. Based on the average summer SST from the World Ocean Atlas (WOA09) data set (Locarnini et al. 2010), the modern sea surface temperature in our study site was about 0–1 °C. For the historical period, the highest subsurface temperature is about 4–5 °C during the Holocene at similar latitudes, including the eastern Antarctic continental margin (Kim et al. 2012) and western Antarctic Peninsula (Etourneau et al. 2013). According to modern observation and SST reconstruction during the late Pleistocene, we suggest that the highest SST in our study site should be lower than 5 °C in the warmer periods, which was much lower than $U^{k'}_{37}$-SST. Therefore, all these results indicating higher $\%C_{37:4}$ are most likely controlled by extremely low SST

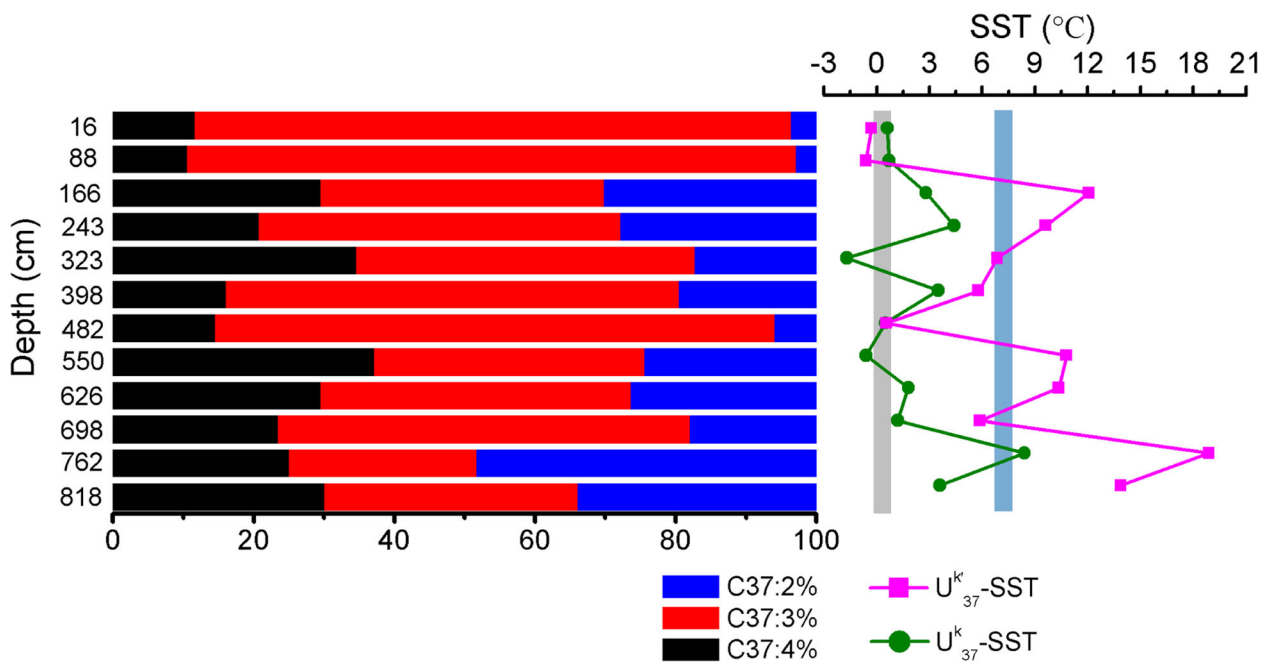

Fig. 6 The relative abundance of $C_{37:4}$, $C_{37:3}$, and $C_{37:2}$ alkenones and the calculated sea surface temperature based on U^{k}_{37} and $U^{k'}_{37}$ index at different depths of the core R23. The light gray and light blue bands represent modern average summer SST based on the World Ocean Atlas (WOA09) data set (Locarnini et al. 2010) and highest SST during the Holocene at the same latitude of the Southern Ocean from previous studies (Kim et al. 2012; Etourneau et al. 2013), respectively

in the R23 sediments, and the U^{k}_{37} index is more feasible than $U^{k'}_{37}$ in the relatively higher latitudes of the Southern Ocean.

Ho et al. (2012) also found that the $U^{k'}_{37}$-SST records were significantly warmer in glacial periods and that the U^{k}_{37} index is a more suitable SST proxy in the sub-Antarctic and higher latitude Pacific (Ho et al. 2012; Haddam et al. 2018). Other studies have shown a significant relationship between the relative abundance of $C_{37:4}$ and temperature (Prahl et al. 1988). Moreover, several other studies indicate $\%C_{37:4}$ is closely related to cold water mass expansion (Bard et al. 2000; Martínez-Garcia et al. 2010). Although the influencing factors on the relative abundance of $C_{37:4}$ alkenone are complex, a statistically significant relationship between U^{k}_{37} index and SST has been found in the surface sediments from high latitudes of the North Atlantic Ocean (Rosell-Melé et al. 1995). This result further validates the general applicability of the U^{k}_{37} as a reliable climatic proxy for SST reconstructions in the relatively cold climate regions (Rosell-Melé et al. 1994, 1995). The latitude was relatively high at our study site, and the modern annual summer SST was lower than 1 °C. The marine algae may synthesize more $C_{37:4}$ alkenones to adapt to the extremely cold conditions. Notably, there are few U^{k}_{37}-SST records in the Southern Ocean at latitudes higher than 60°S. Therefore, all these results indicate that the usage of the U^{k}_{37} index is feasible for reconstructing past SST in the Southern Ocean, but more studies on surface water and sediment samples in high latitudes are required to confirm the relationship between $C_{37:4}$ alkenones and sea surface temperature.

5 Conclusions

We have presented pilot results of the relative distribution and individual $\delta^{13}C$ values of long-chain *n*-alkanes and the organic geochemical characterization of alkenones in 12 samples selected from a sediment core collected from the Pacific sector of the Southern Ocean. Our results suggest that the abundant long-chain *n*-alkanes (C_{27}–C_{35}) with a significant odd-over-even carbon preference might have originated from terrestrial higher plant waxes, possibly via long-range transport of dust from Australia and New Zealand. The mid-chain *n*-alkanes (C_{23}–C_{25}) preserved in the sediments have low odd-over-even carbon preference, perhaps indicating mixing of marine (non-diatom pelagic phytoplankton and marine microalgae) and terrestrial sources. The C_{26} and C_{28} *n*-alkanes with relatively low $\delta^{13}C$ values indicate an origin from marine chemoautotrophic bacteria. The $\delta^{13}C$ values of long-chain *n*-alkanes (C_{27}–C_{31}) range between −30.8 and −24.8‰ in the sediments, approximately 5–10‰ higher than in terrestrial C_3 higher plants. Furthermore, the relative abundance of tetra-unsaturated alkenone in the sediments varies from 11 to 37%, higher than those previously reported in the lower latitudes of the South Pacific Ocean. We conclude that tetra-unsaturated alkenones are sensitive markers of low SSTs, suggesting the feasibility of using U^{k}_{37} in further SST reconstructions in the Pacific sector of the Southern Ocean.

6 Supplementary Information

The online version contains supplementary material available at https://doi.org/10.1186/s40645-021-00416-9.

Additional file 1. Supplementary material.

Acknowledgements

We are grateful to the crew of the R/V Xuelong for their assistance with sample collection in the 31st CHINARE, and thanks to Chinese Projects for Investigations and Assessments of the Arctic and Antarctic (CHINARE2012-2020 for 01-04, 02-01, and 03-04). We also acknowledge Prof. S. Emslie for editing and Prof. Tiegang Li for providing samples. We are grateful to Dr. Yusuke Okazaki and two anonymous reviewers whose comments significantly improved the quality of the manuscript.

Authors' contributions

MC, XL, and XC proposed the topic, conceived and designed the study, and they wrote the draft of this paper. XC and DL conducted the experiments. All the co-authors contributed to the discussion and edited and commented on the paper. All authors read and approved the final manuscript.

Funding

This study was supported by grant numbers 41776188, 41576183, 41476172, and 41772366 from the National Natural Science Foundation of China, and the Fundamental Research Funds for the Central Universities. This work was also partly supported by the Joint Projects of MOST (Ministry of Science and Technology) to MTC and the Chinese Projects for Investigations and Assessments of the Arctic and Antarctic (CHINARE2012-2020 for 01-04, 02-01, and 03-04) to LQC.

Availability of data and materials

The datasets in the current study are available from the corresponding author on reasonable request.

Declarations

Competing interests

The authors declare that they have no competing interests.

Author details

[1]Anhui Province Key Laboratory of Polar Environment and Global Change, School of Earth and Space Sciences, University of Science and Technology of China, Hefei 230026, Anhui, China. [2]Key Laboratory of Global Change and Marine-Atmospheric Chemistry (GCMAC) of Ministry of Natural Resources (MNR), Third Institute of Oceanography (TIO), MNR, Xiamen 361005, China. [3]Institute of Earth Sciences, National Taiwan Ocean University, Keelung 20224, Taiwan. [4]Center of Excellence for the Oceans, National Taiwan Ocean University, Keelung 20224, Taiwan. [5]Center of Excellence for Ocean Engineering, National Taiwan Ocean University, Keelung 20224, Taiwan. [6]Taiwan Ocean Research Institute, National Applied Research Laboratories, Kaohsiung 80143, Taiwan. [7]Key Laboratory of Marine Geology and Metallogeny, First Institute of Oceanography, Ministry of Natural Resources, Qingdao 266061, China. [8]Pilot National Laboratory for Marine Science and Technology, Qingdao 266061, China.

Received: 30 July 2020 Accepted: 5 March 2021
Published online: 06 April 2021

References

Ashley K, Bendle J, Crosta X, Etourneau J, Campagne P, Gilchrist H, Ibraheem U, Greene S, Schmidt S, Eley Y, Massé G (2020) Fatty acid carbon isotopes: a new indicator of marine Antarctic paleoproductivity? Biogeosciences Discuss. [preprint], https://doi.org/10.5194/bg-2020-124, in review, 2020

Bard E, Rostek F, Turon JL, Gendreau S (2000) Hydrological impact of Heinrich events in the subtropical northeast Atlantic. Science 289(5483):1321–1324. https://doi.org/10.1126/science.289.5483.1321

Bendle J, Kawamura K, Yamazaki K, Niwai T (2007) Latitudinal distribution of terrestrial lipid biomarkers and n-alkane compound-specific stable carbon isotope ratios in the atmosphere over the western Pacific and Southern Ocean. Geochim Cosmochim Acta 71(24):5934–5955. https://doi.org/10.1016/j.gca.2007.09.029

Bendle J, Rosell-Melé A, Ziveri P (2005) Variability of unusual distributions of alkenones in the surface waters of the Nordic seas. Paleoceanography 20(2): PA2001. https://doi.org/10.1029/2004PA001025

Brassell SC, Eglinton G, Marlowe IT, Pfaumann U, Sarnthein M (1986) Molecular stratigraphy: a new tool for climatic assessment. Nature 320(6058):129–133. https://doi.org/10.1038/320129a0

Bray EE, Evans ED (1961) Distribution of n-paraffins as a clue to recognition of source beds. Geochim Cosmochim Acta 22(1):2–15. https://doi.org/10.1016/0016-7037(61)90069-2

Bubba MD, Cincinelli A, Checchini L, Lepri L, Desideri P (2004) Horizontal and vertical distributions of biogenic and anthropogenic organic compounds in the Ross Sea (Antarctica). Int J Environ Anal Chem 8:441–456

Chen X, Liu X, Wei Y, Huang Y (2019) Production of long chain n-alkyl lipids by heterotrophic microbes: new evidence from Antarctic lakes. Org Geochem 138:103909. https://doi.org/10.1016/j.orggeochem.2019.103909

Chewings JM, Atkins CB, Dunbar GB, Golledge NR (2014) Aeolian sediment transport and deposition in a modern high-latitude glacial marine environment. Sedimentology 61(6):1535–1557. https://doi.org/10.1111/sed.12108

Chikaraishi Y, Naraoka H (2007) $\delta^{13}C$ and δD relationships among three n-alkyl compound classes (n-alkanoic acid, n-alkane and n-alkanol) of terrestrial higher plants. Org Geochem 38(2):198–215. https://doi.org/10.1016/j.orggeochem.2006.10.003

Cincinelli A, Martellini T, Bittoni L, Russo A, Gambaro A, Lepri L (2008) Natural and anthropogenic hydrocarbons in the water column of the Ross Sea (Antarctica). J Mar Syst 73(1-2):208–220. https://doi.org/10.1016/j.jmarsys.2007.10.010

Collister JW, Lichtfouse E, Hieshima G, Hayes JM (1994) Partial resolution of sources of n-alkanes in the saline portion of the Parachute Creek Member, Green River Formation (Piceance Creek Basin, Colorado). Org Geochem 21(6-7):645–659. https://doi.org/10.1016/0146-6380(94)90010-8

Conte MH, Sicre MA, Rühlemann C, Weber JC, Shultz-Bull D, Blanz T (2006) Global temperature calibration of the alkenone unsaturation index ($U^{K'}_{37}$) in surface waters and comparison with surface sediments. Geochem Geophys Geosyst 7(2):Q02005. https://doi.org/10.1029/2005GC001054

Diefendorf AF, Freimuth EJ (2017) Extracting the most from terrestrial plant -derived n-alkyl lipids and their carbon isotopes from the sedimentary record: a review. Org Geochem 103:1–21. https://doi.org/10.1016/j.orggeochem.2016.10.016

Duan Y, He J (2011) Distribution and isotopic composition of n-alkanes from grass, reed and tree leaves along a latitudinal gradient in China. Geochem J 45(3):199–207. https://doi.org/10.2343/geochemj.1.0115

Duncan B, McKay R, Bendle J, Naish T, Inglis GN, Moossen H, Levy R, Ventura GT, Lewis A, Chamberlain B, Walker C (2019) Lipid biomarker distributions in Oligocene and Miocene sediments from the Ross Sea region, Antarctica: implications for use of biomarker proxies in glacially-influenced settings. Palaeogeogr Palaeoclimatol Palaeoecol 516:71–89. https://doi.org/10.1016/j.palaeo.2018.11.028

Edwards EJ, Osborne CP, Stromberg CA, Smith SA (2010) The origins of C_4 grasslands: integrating evolutionary and ecosystem science. Science 328(5978):587–591. https://doi.org/10.1126/science.1177216

Eglinton TI, Eglinton G (2008) Molecular proxies for paleoclimatology. Earth Planet Sci Lett 275(1-2):1–16. https://doi.org/10.1016/j.epsl.2008.07.012

Etourneau J, Collins LG, Willmott V, Kim JH, Barbara L, Leventer A, Schouten S, Sinninghe Damste JS, Bianchini A, Klien V, Crosta X, Massé G (2013) Holocene climate variations in the western Antarctic Peninsula: evidence for sea ice extent predominantly controlled by changes in insolation and ENSO variability. Clim Past 9(4):1431–1446. https://doi.org/10.5194/cp-9-1431-2013

Fischer H, Schmitt J, Lüthi D, Stocker TF, Tschumi T, Parekh P, Joos F, Köhler P, Völker C, Gersonde R, Barbante C, Le Floch M, Raynaud D, Wolff EW (2010) The role of Southern Ocean processes in orbital and millennial CO_2 variations–a synthesis. Quat Sci Rev 29(1-2):193–205. https://doi.org/10.1016/j.quascirev.2009.06.007

Haddam NA, Siani G, Michel E, Kaiser J, Lamy F, Duchamp-Alphonse S, Hefter J, Braconnot P, Dewilde F, Isgüder G, Tisnerat-Laborde N, Thil F, Durand N, Kissel C (2018) Changes in latitudinal sea surface temperature gradients along the Southern Chilean margin since the last glacial. Quat Sci Rev 194: 62–76. https://doi.org/10.1016/j.quascirev.2018.06.023

Harada N, Handa N, Fukuchi M, Ishiwatari R (1995) Source of hydrocarbons in marine sediments in Lützow-Holm Bay, Antarctica. Org Geochem 23(3):229–237. https://doi.org/10.1016/0146-6380(94)00124-J

Harada N, Sato M, Oguri K, Hagino K, Okazaki Y, Katsuki K, Tsuji Y, Shin KH, Tadai O, Saitoh SI, Narita H, Konno S, Jordan RW, Shiraiwa Y, Grebmeier J (2012) Enhancement of coccolithophorid blooms in the Bering sea by recent environmental changes. Glob Biogeochem Cycles 26(2):GB2036. https://doi.org/10.1029/2011GB004177

Harada N, Sato M, Shiraishi A, Honda MC (2006) Characteristics of alkenone distributions in suspended and sinking particles in the northwestern North Pacific. Geochim Cosmochim Acta 70(8):2045–2062. https://doi.org/10.1016/j.gca.2006.01.024

Hayakawa K, Handa N, Ikuta N, Fukuchi M (1996) Downward fluxes of fatty acids and hydrocarbons during a phytoplankton bloom in the austral summer in Breid Bay, Antarctica. Org Geochem 24(5):511–521. https://doi.org/10.1016/0146-6380(96)00047-2

Hayes JM, Freeman KH, Popp BN, Hoham CH (1990) Compound-specific isotopic analyses: a novel tool for reconstruction of ancient biogeochemical processes. Org Geochem 16(4-6):1115–1128. https://doi.org/10.1016/0146-6380(90)90147-R

Ho SL, Mollenhauer G, Lamy F, Martinez-Garcia A, Mohtadi M, Gersonde R, Hebbeln D, Nunez-Ricardo S, Rosell-Mele A, Tiedemann R (2012) Sea surface temperature variability in the Pacific sector of the Southern Ocean over the past 700 kyr. Paleoceanography 27(4):PA4202. https://doi.org/10.1029/2012PA002317

Holtvoeth J, Whiteside JH, Engels S, Freitas FS, Grice K, Greenwood P, Johnson S, Kendall I, Lengger SK, Lücke A, Mayr C, Naafs BDA, Rohrssen M, Sepúlveda J (2019) The paleolimnologist's guide to compound-specific stable isotope analysis – an introduction to principles and applications of CSIA for quaternary lake sediments. Quat Sci Rev 207:101–133. https://doi.org/10.1016/j.quascirev.2019.01.001

Huang Y, Eglinton G, Ineson P, Latter PM, Bol R, Harkness DD (1997) Absence of carbon isotope fractionation of individual n-alkanes in a 23-year field decomposition experiment with Calluna vulgaris. Org Geochem 26(7-8):497–501. https://doi.org/10.1016/S0146-6380(97)00027-2

Huang Y, Street-Perrott FA, Metcalfe SE, Brenner M, Moreland M, Freeman K (2001) Climate change as the dominant control on glacial-interglacial variations in C_3 and C_4 plant abundance. Science 293(5535):1647–1651. https://doi.org/10.1126/science.1060143

Ishiwatari R, Uzaki M, Yamada K (1994) Carbon isotope composition of individual n-alkanes in recent sediments. Org Geochem 21(6-7):801–808. https://doi.org/10.1016/0146-6380(94)90021-3

Jaeschke A, Wengler M, Hefter J, Ronge TA, Geibert W, Mollenhauer G, Lamy F (2017) A biomarker perspective on dust, productivity, and sea surface temperature in the Pacific sector of the Southern Ocean. Geochim Cosmochim Acta 204:120–139. https://doi.org/10.1016/j.gca.2017.01.045

Kim JH, Crosta X, Willmott V, Renssen H, Bonnin J, Helmke P, Schouten S, Sinninghe Damste JS (2012) Holocene subsurface temperature variability in the eastern Antarctic continental margin. Geophys Res Lett 39(6):L06705. https://doi.org/10.1029/2012GL051157

Kohfeld KE, Graham RM, De Boer AM, Sime LC, Wolff EW, Le Quéré C, Bopp L (2013) Southern hemisphere westerly wind changes during the Last Glacial Maximum: paleo-data synthesis. Quat Sci Rev 68:76–95. https://doi.org/10.1016/j.quascirev.2013.01.017

Kvenvolden KA, Rapp JB, Golan-Bac M, Hostettler FD (1987) Multiple sources of alkanes in quaternary oceanic sediment of Antarctica. Org Geochem 11(4): 291–302. https://doi.org/10.1016/0146-6380(87)90040-4

Lamy F, Gersonde R, Winckler G, Esper O, Jaeschke A, Kuhn G, Ullermann J, Martínez-Garcia A, Lambert F, Kilian R (2014) Increased dust deposition in the Pacific Southern Ocean during glacial periods. Science 343(6169):403–407. https://doi.org/10.1126/science.1245424

Lamy F, Kilian R, Arz HW, Francois JP, Kaiser J, Prange M, Steinke T (2010) Holocene changes in the position and intensity of the southern westerly wind belt. Nat Geosci 3(10):695–699. https://doi.org/10.1038/ngeo959

Lewis AR, Ashworth AC (2016) An early to middle Miocene record of ice-sheet and landscape evolution from the Friis Hills, Antarctica. Geol Soc Am Bull 128(5-6):719–738. https://doi.org/10.1130/B31319.1

Lewis AR, Marchant DR, Ashworth AC, Hedenaes L, Hemming SR, Johnsons JV, Leng MJ, Machlus ML, Newton AE, Raine JI, Willenbring JK, Williams M, Wolfe AP (2008) Mid-Miocene cooling and the extinction of tundra in continental Antarctica. Proc. Natl. Acad. Sci. U.S.A 105: 10676-10680

Li R, Fan J, Xue J, Meyers PA (2017) Effects of early diagenesis on molecular distributions and carbon isotopic compositions of leaf wax long chain biomarker n-alkanes: comparison of two one-year-long burial experiments. Org Geochem 104:8–18. https://doi.org/10.1016/j.orggeochem.2016.11.006

Locarnini RAM, Antonov JI, Boyer TP, Garcia HE, Baranova OK, Zweng MM, Johnson DR (2010) World Ocean Atlas 2009: Volume 1: Temperature. In NOAA Atlas NESDIS 68 (ed. S. Levitus). U.S. Government Printing Office, Washington D.C. p. 184

Marshall J, Speer K (2012) Closure of the meridional overturning circulation through Southern Ocean upwelling. Nat Geosci 5(3):171–180. https://doi.org/10.1038/ngeo1391

Martínez-Garcia A, Rosell-Melé A, Geibert W, Gersonde R, Masqué P, Gaspari V, Barbante C (2009) Links between iron supply, marine productivity, sea surface temperature, and CO_2 over the last 1.1 Ma. Paleoceanography 24(1): PA1207. https://doi.org/10.1029/2008PA001657

Martínez-Garcia A, Rosell-Melé A, Jaccard SL, Geibert W, Sigman DM, Haug GH (2011) Southern Ocean dust–climate coupling over the past four million years. Nature 476(7360):312–315. https://doi.org/10.1038/nature10310

Martinez-Garcia A, Rosell-Mele A, McClymont EL, Gersonde R, Haug GH (2010) Subpolar Link to the Emergence of the Modern Equatorial Pacific Cold Tongue. Science 328 (5985):1550–1553

Matsumoto GI, Honda E, Sonoda K, Yamamoto S, Takemura T (2010) Geochemical features and sources of hydrocarbons and fatty acids in soils from the McMurdo Dry Valleys in the Antarctic. Polar Sci 4(2):187–196. https://doi.org/10.1016/j.polar.2010.04.001

Meyers PA, Ishiwatari R (1993) Lacustrine organic geochemistry—an overview of indicators of organic matter sources and diagenesis in lake sediments. Org Geochem 20(7):867–900. https://doi.org/10.1016/0146-6380(93)90100-P

Naraoka H, Ishiwatari R (2000) Molecular and isotopic abundances of long-chain n-fatty acids in open marine sediments of the western North Pacific. Chem Geol 165(1-2):23–36. https://doi.org/10.1016/S0009-2541(99)00159-X

Neff PD, Bertler NAN (2015) Trajectory modeling of modern dust transport to the Southern Ocean and Antarctica. J Geophys Res Atmos 120(18):9303–9322. https://doi.org/10.1002/2015JD023304

Nylen TH, Fountain AG, Doran PT (2004) Climatology of katabatic winds in the McMurdo dry valleys, southern Victoria Land, Antarctica. J Geophys Res Atmos 109(D3):D03114. https://doi.org/10.1029/2003JD003937

Ohkouchi N, Kawamura K, Takemoto N, Ikehara M, Nakatsuka T (2000) Implications of carbon isotope ratios of C_{27}-C_{33} alkanes and C_{37} alkenes for the sources of organic matter in the Southern Ocean surface sediments. Geophys Res Lett 27(2):233–236. https://doi.org/10.1029/1999GL002351

Pahnke K, Zahn R (2005) Southern hemisphere water mass conversion linked with North Atlantic climate variability. Science 307(5716):1741–1746. https://doi.org/10.1126/science.1102163

Poynter J, Eglinton G (1990) Molecular composition of three sediments from Hole 717C: the Bengal Fan. In: Cochran JR, Stow DAV et al (eds) Proceedings of Ocean Drilling Program, Scientific Results, vol 166. TX (Ocean Drilling Program), College Station, pp 155–161

Prahl FG, Muehlhausen LA, Zahnle DL (1988) Further evaluation of long-chain alkenones as indicators of paleoceanographic conditions. Geochim Cosmochim Acta 52(9):2303–2310. https://doi.org/10.1016/0016-7037(88)90132-9

Prahl FG, Wakeham SG (1987) Calibration of unsaturation patterns in long-chain ketone compositions for palaeotemperature assessment. Nature 330(6146): 367–369. https://doi.org/10.1038/330367a0

Rosell-Melé A, Carter J, Eglinton G (1994) Distributions of long-chain alkenones and alkyl alkenoates in marine surface sediments from the North East Atlantic. Org Geochem 22(3-5):501–509. https://doi.org/10.1016/0146-6380(94)90122-8

Rosell-Melé A, Eglinton G, Pflaumann U, Sarnthein M (1995) Atlantic core-top calibration of the U^{K}_{37} index as a sea-surface palaeotemperature indicator. Geochim Cosmochim Acta 59(15):3099–3107. https://doi.org/10.1016/0016-7037(95)00199-A

Shevenell AE, Ingalls AE, Domack EW, Kelly C (2011) Holocene Southern Ocean surface temperature variability west of the Antarctic Peninsula. Nature 470(7333):250–254. https://doi.org/10.1038/nature09751

Sicre MA, Bard E, Ezat U, Rostek F (2002) Alkenone distributions in the North Atlantic and Nordic sea surface waters. Geochem Geophys Geosyst 3(2):1 of 13–13 of 13. https://doi.org/10.1029/2001GC000159

Sikes EL, Sicre MA (2002) Relationship of the tetra-unsaturated C_{37} alkenone to salinity and temperature: implications for paleoproxy applications. Geochem Geophys Geosyst 3. https://doi.org/10.1029/2001GC000159

Sikes EL, Volkman JK (1993) Calibration of alkenone unsaturation ratios ($U^{k'}_{37}$) for paleotemperature estimation in cold polar waters. Geochim Cosmochim Acta 57(8):1883–1889. https://doi.org/10.1016/0016-7037(93)90120-L

Sikes EL, Volkman JK, Robertson LG, Pichon JJ (1997) Alkenones and alkenes in surface waters and sediments of the Southern Ocean: implications for paleotemperature estimation in polar regions. Geochim Cosmochim Acta 61(7):1495–1505. https://doi.org/10.1016/S0016-7037(97)00017-3

Theissen KM, Dunbar RB, Cooper AK, Mucciarone DA, Hoffmann D (2003) The Pleistocene evolution of the East Antarctic Ice Sheet in the Prydz Bay region: stable isotopic evidence from ODP Site 1167. Glob Planet Chang 39(3-4):227–256. https://doi.org/10.1016/S0921-8181(03)00118-8

Thomas EK, Huang Y, Morrill C, Zhao J, Wegener P, Clemens SC, Colman SM, Gao L (2014) Abundant C_4 plants on the Tibetan Plateau during the late glacial and early Holocene. Quat Sci Rev 87:24–33. https://doi.org/10.1016/j.quascirev.2013.12.014

Tiedemann R (2012) FS Sonne Fahrtbericht/Cruise Report SO213. Alfred Wegener Institute, Bremerhaven

Toggweiler JR, Russell J (2008) Ocean circulation in a warming climate. Nature 451(7176):286–288. https://doi.org/10.1038/nature06590

Toyos MH, Lamy F, Lange CB, Lembke-Jene L, Saavedra-Pellitero M, Esper O, Arz HW (2020) Antarctic circumpolar current dynamics at the Pacific entrance to theDrake Passage over the past 1.3 millionyears. Paleoceanography and Paleoclimatology 35:e2019PA003773. https://doi.org/10.1029/2019PA003773

Venkatesan MI (1988) Organic geochemistry of marine sediments in Antarctic region: marine lipids in McMurdo Sound. Org Geochem 12(1):13–27. https://doi.org/10.1016/0146-6380(88)90111-8

Vogts A, Moossen H, Rommerskirchen F, Rullkötter J (2009) Distribution patterns and stable carbon isotopic composition of alkanes and alkan-1-ols from plant waxes of African rain forest and savanna C_3 species. Org Geochem 40(10): 1037–1054. https://doi.org/10.1016/j.orggeochem.2009.07.011

Volkman JK, Barrett SM, Blackburn SI, Mansour MP, Sikes EL, Gelin F (1998) Microalgal biomarkers: a review of recent research developments. Org Geochem 29(5-7):1163–1179. https://doi.org/10.1016/S0146-6380(98)00062-X

Wu L, Wang R, Wenshen X, Shulan G, Zhihua C (2015) High resolution age model of Late Quaternary mouth fan at Prydz trough, Eastern Antarctic. Marine Geology and Quaternary Geology (in Chinese with English abstract) 35:197–208

Yamamoto M, Shiraiwa Y, Inouye I (2000) Physiological responses of lipids in *Emiliania huxleyi* and *Gephyrocapsa oceanica* (Haptophyceae) to growth status and their implications for alkenone paleothermometry. Org Geochem 31(9):799–811. https://doi.org/10.1016/S0146-6380(00)00080-2

Zech M, Pedentchouk N, Buggle B, Leiber K, Kalbitz K, Marković SB, Glaser B (2011) Effect of leaf litter degradation and seasonality on D/H isotope ratios of n-alkane biomarkers. Geochim Cosmochim Acta 75(17):4917–4928. https://doi.org/10.1016/j.gca.2011.06.006

Publisher's Note